Asian Review of Mechanical Engineering
ISSN: 2249-6289 (P) Vol.3 No.2, 2014, pp.59-64

DOI: https://doi.org/10.51983/arme-2014.3.2.2375

Corrosion Studies of Thermal Sprayed HA and HA+Al_2O_3-TiO_2 Coatings on 316L Stainless Steel

Bhupesh Walia[1*], T.P Singh Sarao[1] and J.S Grewal[2]
[1]Department of Mechanical Engineering, GCE, Khanna, Punjab, India
[2]Department of Production Engineering, GNDEC, Ludhiana, Punjab, India
* corresponding author e-mail: walia.bhupesh@gmail.com

Abstract - This study was performed to evaluate corrosion behavior of thermal sprayed hydroxyapatite (HA) and hydroxyapatite+Alumina-titania (HA+Al_2O_3-TiO_2) coatings on 316L stainless steel (316L SS) implant material. HA powder was mixed with Al_2O_3-TiO_2 in 60:40 wt. % for depositing HA+Al_2O_3-TiO_2 composite coatings. The coatings were characterized by X-ray diffraction (XRD) and scanning electron microscopy (SEM)/energy-dispersive X-ray spectroscopy (EDS) analyses. Tafel and Potentiodynamic techniques were used to access the in-vitro corrosion behavior of two coatings and un-coated 316L SS in Hank's solution. The corrosion resistance of 316L SS showed a significant improvement after the deposition of coatings.

Keywords: Corrosion, Thermal Spraying, HA+Al_2O_3-TiO_2, Hank's Solution.

I.INTRODUCTION

Metals with excellent mechanical properties and reasonable biocompatibility are widely used as implants. Biomedical implants are usually made of metallic materials, such as austenitic stainless steel, cobalt–chromium alloys, and titanium and its alloys. Among all the metallic materials, ASTM recommended surgical grade 316L SS is the most popular materials because of their relative low cost, increased mechanical strength, ease of fabrication and reasonable corrosion resistance. 316L SS is widely used for prosthesis devices such as bone plates, screw, etc., in orthopedics [1, 2].

The two major issues regarding the long term use of metallic implants in highly aggressive human body environment are corrosion of metallic implants and the lack of integration of metallic implants with human tissues [3]. Corrosion of 316L SS has been a subject of extensive research. It is reported that stainless steel is often susceptible to pitting corrosion. Oxide film on the stainless steel surface consists of inner chromium oxide layer and outer nickel oxide layer. However, when these materials are used in highly rigorous human body environment, their degradation takes place and corrosion products of iron, chromium nickel and molybdenum releases in the body. It is reported that nickel and chromium can cause allergic problems due to their toxic effects [4].

Surface coating can be an attractive solution to reduce the release of metal ions from stainless steels. Surface coatings change the biomaterials' surface composition, structure and morphology, retaining their bulk mechanical properties as such [5]. Al_2O_3-TiO_2 has attracted attention as a composite or bond coat material because of its biological and corrosion resistance effects [6]. In this work, the corrosion behavior has been investigated by Tafel extrapolation and cyclic polarization methods in simulated body fluid (Hank's solution).

II.MATERIALS AND METHODS

A.Feedstock Powder And Substrate

A commercially available HA, Al_2O_3, TiO_2 powders were used in this study. Commercially available biomedical material, stainless steel (316L SS) with chemical composition in weight %-C: 0.024; Cr: 16.850; Ni: 10.735; Mo: 2.269; Si: 0.468; Mn: 1.156; P: 0.032; S: 0.017 and Fe: balance was used as the substrate in this study. 316L SS coupons, each measuring 20mm x 15mm x 2mm were prepared. The specimens were polished by different grades of silicon carbide papers followed by cloth wheel polishing with alumina paste, on a polishing machine. These specimens were cleaned in acetone followed by air drying. The substrates were then grit blasted using alumina (Al_2O_3) grits.

B.Development of Coatings

The 316L SS specimens were thermal sprayed using flame spray system (CERAJET) at Metalizing Equipment Company Private Limited (MECPL), Jodhpur, India**.** In this system, acetylene and oxygen were used as combustion gases and air was used as the carrier gas to feed the powder from hooper to the spray torch. This system is a high velocity version of flame spraying system and is specially designed for ceramic coatings. The spraying parameters used for the deposition of coatings are given in Table 1.

TABLE 1 THERMAL SPRAY PROCESS PARAMETERS FOR DEPOSITION COATINGS

Spraying Parameter		Value
Acetylene flow rate	(l min^{-1})	73
Oxygen flow rate	(l min^{-1})	44
Air pressure	(kg cm^{-2})	4.5
Powder feed rate	(g min^{-1})	15
Spray distance	(cm)	10

C.*Characterization of Powders and Sprayed Coatings*

Coated samples were characterized using XRD and SEM/EDS techniques. The phase composition of the starting powder as well as the as-sprayed coatings was analyzed by an x-ray diffractometer (X'pert-PRO, Make Netherland) with Cu-Kα radiation, operating at 40 KV/30 mA. The coated samples were scanned over 2θ range of 20-60°. The morphology of feedstock powders HA and

HA+Al_2O_3-TiO_2 coatings was examined by SEM (QUANTA 200 FEG, Make: FEl Netherlands) coupled with EDS. After surface characterization, the samples were sectioned with a low speed precision saw at 75 rpm speed and mounted in epoxy resin using specimen mounting press. Mounted samples were polished with emery papers of 220, 400, 600 and 800 grade and subsequently 1/0, 2/0, 3/0 and 4/0 grades. Then samples were grounded and mirror polished with slurry of alumina on a napped cloth to highlight the surface of HA and HA+Al_2O_3-TiO_2 coated substrates. The samples were gold plated to achieve the desired conductivity before observation in scanning electron microscope. Surface as well as cross-sectional SEM/EDS analysis of the coated samples was done to study their elemental compositions along with micro structural features.

D. Electrochemical Corrosion Studies

To investigate the electrochemical corrosion behavior of the uncoated, HA and HA+Al_2O_3-TiO_2 coated 316L SS specimens, potentiodynamic polarization tests were conducted using a Potentiostat/Galvanostat (Series G-750; Gamry Instruments, Inc. USA), interfaced to a computer and supported with Gamry electrochemical software DC105. The electrolyte used for simulating human body fluid conditions was Hank's solution with chemical composition (in g/l) 0.14 $CaCl_2$, 0.40 KCL, 0.60 KH_2PO_4, 0.60 $MgCl_2$-$6H_2O$, 0.06 $MgSO_4$-$7H_2O$, 8.00 NaCl, 0.35 $NaHCO_3$, 0.06 Na_2HPO_4 and Glucose 1.0 at pH 6.8. Before conducting the corrosion studies, each specimen was immersed in Hank's solution for 24 hours for stabilization. The exposed area of the samples in the Hank's solution was 1.5 cm^2. The 316L SS specimen forms the working electrode. All potentials were measured with respect to a saturated calomel electrode (SCE) as the reference electrode. A graphite rod served as the counter electrode. All the tests were performed at a scan rate of 1mV/sec and fresh solution was used for each experiment. Polarization curves were initiated at -250 mV below the open circuit potential and the tests were started after a steady open circuit potential was achieved (not more than ± 5mV drift in 5 min). The corrosion rate was determined using the Tafel extrapolation method and all the tests were carried out on three fresh samples to verify reliability of test results.

III.RESULTS AND DISCUSSION

A.*XRD Analysis of Powder*

The XRD scans of HA and Al_2O_3-TiO_2 powders are shown in Fig.1 and Fig. 2 respectively. The scans (Fig.1) indicate that all the major peaks belong to HA as per JCPDS card no. 9-432 and powder is highly crystalline. The analysis Al_2O_3-TiO_2 shows that the entire major peaks belong to Al_2O_3 and TiO_2 rutile phase. TiO_2 crystallizes in three major structures: rutile (tetragonal), anatase (tetragonal), and brookite (rhombohedrical) [6]. Out of three polymorphic forms of titania, rutile is the only stable phase, whereas anatase and brookite are metastable and are transformed to rutile irreversibly by heating [7].

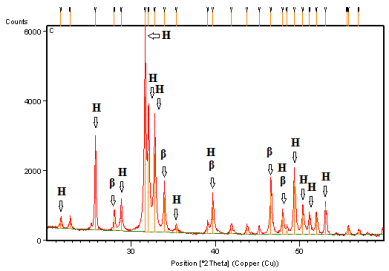

Fig. 1: XRD profile of HA powder [HA (H), and β-TCP]

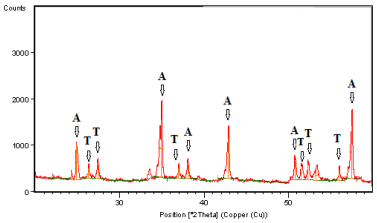

Fig. 2: XRD profile of Al2O3-TiO2 powder [Al2O3 (A), and TiO2 rutile (T)]

B.SEM/EDS Analysis

The morphology of the feedstock powders is shown in Fig. 3 and Fig. 4 respectively. The SEM micrographs show that HA powder particles have irregular morphology with average particles size of 20 µm. EDS analysis of powder at three different points confirms the presence of Ca, P and O elements. These elements verify that powder is HA. SEM image of Al_2O_3 and TiO_2 powders showed a wide particle size distribution with an average particle size of 30 µm. The typical shape of the powder had an angular morphology of dense solid particles (Fig. 4). It is worthwhile to mention that the particle shape, size and morphology influence the final microstructure of the thermal sprayed coatings.

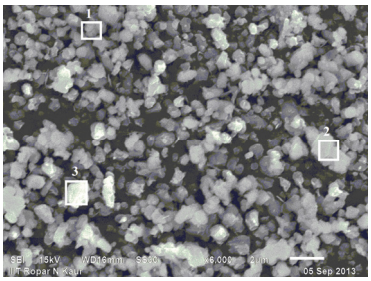

Fig. 3: SEM analysis of HA powder

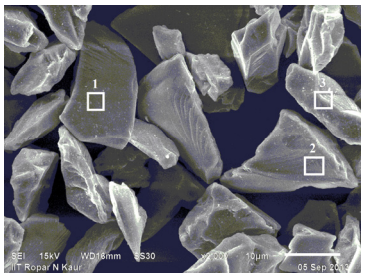

Fig. 4: SEM analysis of Al2O3-TiO2 powder

The SEM micrograph along with EDS point analysis of Al_2O_3-TiO_2 coated specimen is shown in Fig. 5. EDS point analysis of Al_2O_3-TiO_2 coating at different points indicates the presence of Ti and O elements with their relative atomic % values.

IV.CHARACTERIZATION OF AS-SPRAYED COATING

A.XRD Analysis of Coatings

The XRD profile for the thermal sprayed HA coating on 316L substrate is shown in Fig. 5. A very high intensity peak was observed at 31.9° (2θ). XRD analysis of HA coatings showed that coatings are highly crystalline. The analysis of the HA coating confirmed the presence of HA, with minor peaks for tetra-calcium phosphate (TTCP) and β-tri-calcium phosphate (β-TCP) phases. The peaks for TTCP and β-TCP phases are compared with standard JCPDS cards 25-1137 and 9-169, respectively. The decomposition of HA occurs into different phases such as TTCP and TCP is related to the high temperature in thermal spraying flame. Chen et al. (2003) in subsonic thermal sprayed HA coatings reported that dehydroxylation of HA leads to TTCP and TCP phases. It is reported that the amorphous and other non-HA phases enhance dissolution; however there still exists the conflict about the effect of the amorphous phases on mechanical behavior of HA coatings [7]. The phase composition of the thermal sprayed HA+(Al_2O_3-TiO_2) composite coating on 316L SS is shown in Fig. 6 respectively. The coating structure mainly comprises HA (H), Al_2O_3 (A) and TiO_2 rutile (T) phases, with minor TTCP (T*) and α-TCP (α) phases. XRD peaks in Fig. 6 at 32.9° and 46.9° (2θ) indicates the presence of both HA (H) and Al_2O_3 (A) according to JCPDS cards 9-432 and card no. 83-2080. The other peaks TiO_2 rutile (T) and HA (H) are shown at 39° and 41° (2θ) and the major peak is observed at 36° (2θ) of TiO2 rutile (T) as per JCPDS card no. 21-1276.

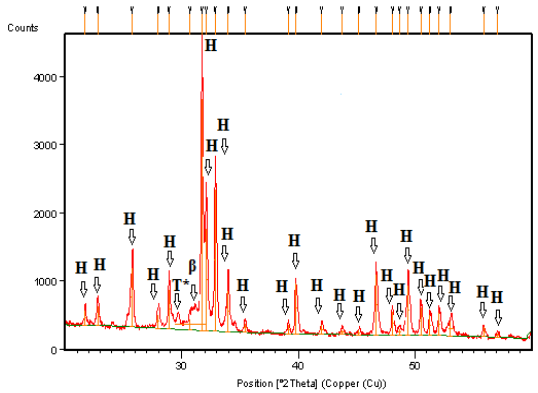

Fig. 5: XRD pattern of thermal sprayed HA coating on 316L SS [HA (H), TTCP (T*), and β-TCP (β)]

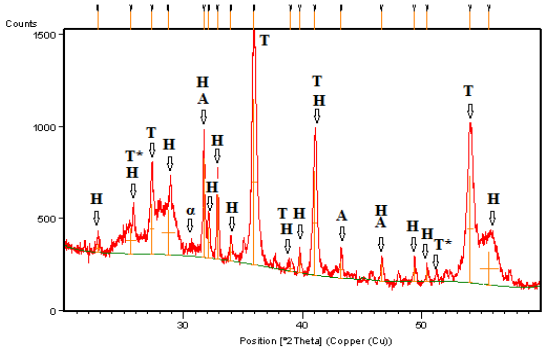

Fig. 6: XRD pattern of thermal sprayed [HA+(Al2O3-TiO2)] composite coating on 316L SS [HA (H), TTCP (T*), Al2O3 (A), TiO2 rutile (T), and α-TCP (α)]

B.SEM/EDS Analysis

The SEM along with EDS point analysis showing elemental composition of thermal sprayed HA coating on 316L SS is shown in Fig. 7. The SEM analysis indicates that the HA coating consists of some tiny spherical and interconnected splats. The coating layer is characterized by some pores and interlamellar micro cracks. The EDS analysis at 1, 2 and 3 (Fig. 4.9) confirms the presence of Ca, P and O.

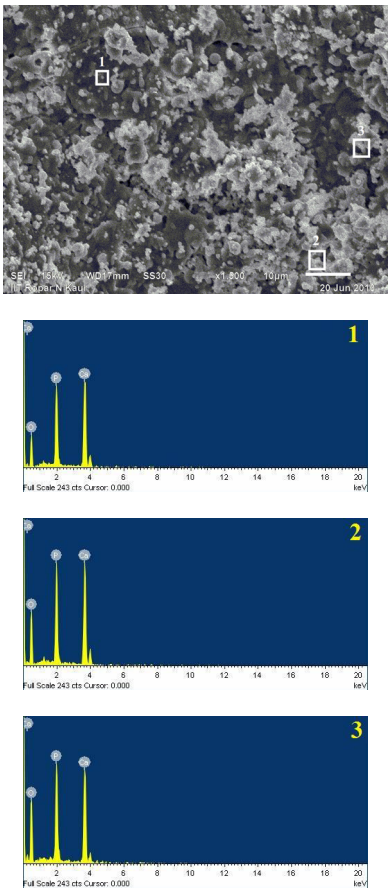

Fig. 7: FE-SEM analysis along with EDS point analysis of thermal sprayed HA coating on 316L SS

SEM morphology of HA+(Al_2O_3-TiO_2) composite coating is shown in Fig. 8. EDS point analysis in area 1, area 2 and area 3 shows the presence of Ca, P, O, Al and Ti elements at different points in the HA+(Al_2O_3-TiO_2) composite coating. Ca, P and O are basic elements of HA coating. Investigation of both HA as well as (Al_2O_3-TiO_2) seem to be well-distributed throughout the HA+(Al_2O_3-TiO_2) coatings microstructure. Point analysis shows that Ca, P, Al and Ti elements coexist in in some melted particles.

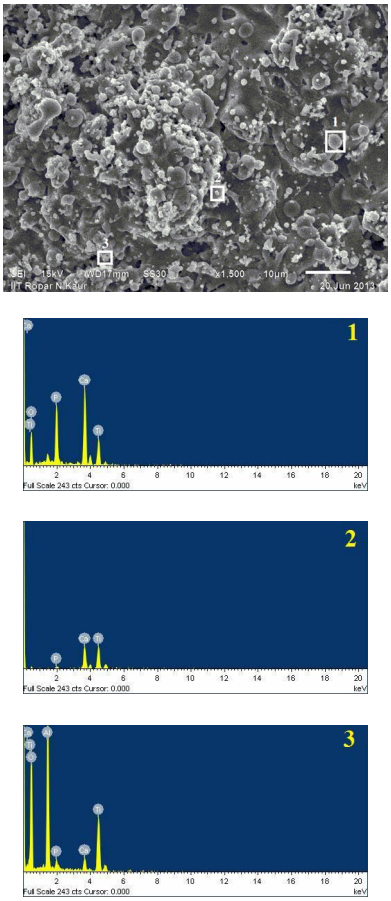

Fig. 8: FE-SEM analysis along with EDS point analysis showing the elemental composition of thermal sprayed HA+(Al2O3-TiO2) composite coating on 316L SS

C.Cross-Section Analysis

The cross-sectional EDS elemental map of polished cross-section of thermal sprayed HA coating on the 316L SS is shown in Fig. 9. The average value of the coating thickness was found from cross-sectional micrograph is to be in range of 100-120 µm. The coating has a typical splat-like laminar morphology. As shown in cross-section of coating, due to brittle nature of ceramic coatings, there is a possibility of some coating particles getting removed during sample preparation.

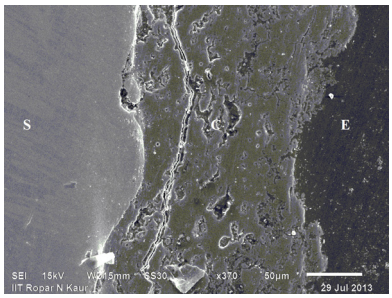

Fig. 9: Cross-sectional SEM of thermal sprayed HA coating on 316L SS (Scale bar = 50 µm)

Cross-sectional HA+(Al_2O_3-TiO_2) composite coating on 316L SS substrate (Fig. 10) indicates that the coating has splat-like lamellar microstructure. The average coating thickness was found from the SEM micrograph to be in a average range of 80 µm. EDS was used to differentiate between the HA and (Al_2O_3-TiO_2) in the HA+(Al_2O_3-TiO_2) composite coating. The coating mainly contains Ca, P, Al and Ti elements.

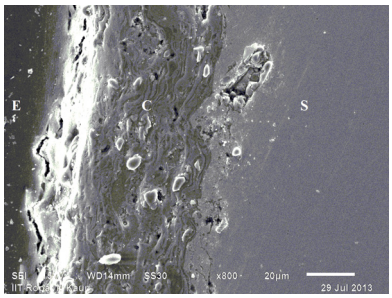

Fig. 10: Cross-sectional SEM of thermal sprayed HA+(Al2O3-TiO2) composite coating on 316L SS (scale bar = 20 µm)

V.SURFACE ROUGHNESS

Surface topography plays a significant role in the improvement of coating adhesion [9]. Rough-surfaced implants favor both bone anchoring and biomechanical stability [10]. The surface roughness parameters (Ra, Rq and Rz) for alumina blasted, HA coated and HA+Al_2O_3-TiO_2 composite coated substrates 316L SS are shown in Fig. 11. The average Ra value for blasted 316L SS substrates was 5.9 µm whereas in HA coated 316L SS it was 5.7 µm.

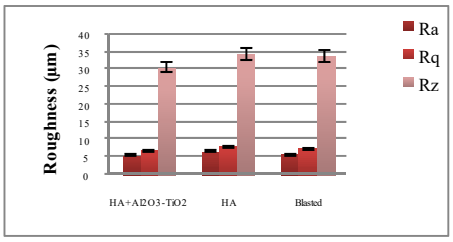

Fig. 11: Graphical representation of surface roughness results for the (1) HA+Al2O3-TiO2 (2) HA and Uncoated coated 316L SS substrates

VI.CORROSION BEHAVIOUR

The potentiodynamic curves of un-coated, HA coated and HA+Al_2O_3-TiO_2 composite coted 316L SS in Hank's solution at 37±1℃ temperature are shown in Fig. 12. The corrosion parameters determined from these curves by Tafel extrapolation method are summarized in Table 2. The various corrosion parameters are anodic tafel slope (β_a), cathodic tafel slope (β_c), corrosion potential (E_{Corr}) and corrosion current density (I_{Corr}). The corrosion potential (E_{Corr}) and corrosion current density (I_{Corr}) are given by inter-section point of the cathodic tafel and the anodic tafel slope. It is well known that corrosion current density (I_{Corr}) is representative of the degree of degradation of metallic material. The higher the corrosion current density (I_{Corr}) at a given potential, the more prone is the material to corrode.

According to the analysis of Tafel slope values, the results show that corrosion current density of uncoated 316L SS in Hank's solution (I_{Corr}= 946 µA) is higher than the HA coated and HA+Al_2O_3-TiO_2 samples (I_{Corr}= 447 nA, and I_{Corr}= 229 nA) respectively. It indicates the susceptibility of the bare 316L SS towards corrosion attack after immersion in Hank's solution. However, the low I_{Corr} values for the HA+Al_2O_3-TiO_2 composite coated samples indicate that the HA+Al_2O_3-TiO_2 coating prevent the substrate surface from corrosion attack during their immersion in Hank's solution. It means that the HA+Al_2O_3-TiO_2 coated samples (I_{Corr}= 229 nA, E_{Corr}= -305 mV) is more corrosion resistant than uncoated 316L SS (I_{Corr}= 946 µA, E_{Corr}= -422 mV) in Hank's solution. These results are consistent with previous corrosion studies on HA coatings [11, 12]. The two layer coating composed of HA/Ti on 316L SS was reported to be more corrosion resistant than the single HA layer on SS316L [13]. In another plasma spray HA coated study, Ti and 316L SS specimens showed a significant effect on corrosion resistance in comparison to un-coated Ti and 316L SS substrates [14]. It shows that HA+Al_2O_3-TiO_2 coating could be a viable alternative for improving the corrosion resistance of 316L SS.

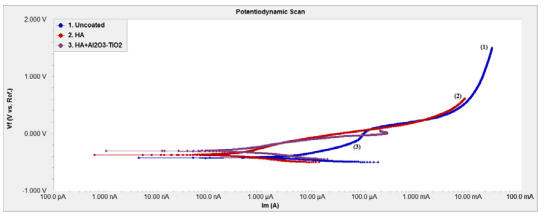

Fig. 12 Potentiodynamic curves of (1) uncoated (2) HA coated and HA+Al_2O_3-TiO_2 composite coated 316L SS in Hank's solution at 37±1℃.

TABLE 2 CORROSION PARAMETERS OF UNCOATED AND HA COATED 316L SS

Parameters		Uncoated	HA coated	HA+Al_2O_3-TiO_2
β_a	(e^{-3}	98.70	346.6	132.2
β_c	(e^{-3}	47.0	119.6	53.2
E_{Corr} (mV)		-422.0	-374.0	-305.0
I_{Corr} (µA)		946.0	0.447	0.229

VII. CONCLUSIONS

In the present study, the corrosion behavior of uncoated, HA coated and HA+Al_2O_3-TiO_2 composite coated 316L SS implant material was evaluated by electrochemical techniques. HA and HA+Al_2O_3-TiO_2 coatings were developed by thermal spray technique. The following conclusions have been drawn from the study:

1. XRD analysis of HA coatings confirmed that all the major peaks belongs to HA, with minor presence of TTCP and β-TCP phases. SEM micrographs of HA coating consist of some tiny spherical and interconnected splats. The coating layer is characterized by some pores and interlamellar micro cracks. The EDS analysis confirms the presence of Ca, P and O compounds in the HA coating.
2. EDS point analysis shows the presence of Ca, P, O, Al and Ti elements at different points in the HA+(Al_2O_3-TiO_2) composite coating. Ca, P and O are basic elements of HA coating. Investigation of both HA as well as (Al_2O_3-TiO_2) seem to be well-distributed throughout the HA+(Al_2O_3-TiO_2) coatings microstructure. Point analysis shows that Ca, P, Al and Ti elements coexist in in some melted particles.
3. Based on the experimental results of Tafel, HA+Al_2O_3+TiO_2 composite coated 316L SS exhibits better corrosion resistance than HA coated and uncoated 316L SS in Hank's solution. It can be deduced that HA and HA+Al_2O_3-TiO_2 coatings prevents the ion release from 316L SS into human body and also decrease its susceptibility to pitting corrosion, providing a great potential in biomedical applications.

REFERENCES

[1] Yilmaz, S. Ipek, M. Celebi, G.F. and Bindal, C. (2005), "The effect of bond coat on mechanical properties of plasma-sprayed Al_2O_3 and Al_2O_3-13 wt% TiO_2 coatings on AISI 316L stainless steel", Vacuum, Vol. 77 (3), pp 315-321.

[2] Niinomi, M. (2003), "Recent research and development in titanium alloys for biomedical applications and healthcare goods", Science and Technology of Advanced Materials", Vol. 4 (5), pp 445-454.

[3] Fathi, M.H. and Doostmohammadi, A. (2009), "Bioactive Glass Nanopowder and Bioglass Coating for Biocompatibility Improvement of Metallic Implant", Journal of Materials Processing Technology, Vol. 209 (3), pp 1385-1391.

[4] Songür, M. Celikkan, H. Gökmeşe, F. Şimşek, S.A. Altun, N.S. and Aksu, M.L. (2009), "Electrochemical corrosion properties of metal alloys used in orthopedic implants", Journal of Applied Electrochemistry, Vol. 39 (3), pp 1259-1265.

[5] Manivasagam, G. Dhinasekaran, D. and Rajamanickam, A. (2010), "Biomedical Implants:Corrosion and its Prevention", Recent Patents on Corrosion Science, Vol. 2, pp 40-54.

[6] Ye, F.X. Ohmori, A. Tsumura, T. Nakata, K. and Li, C.J. (2007), "Microstructural Analysis and Photocatalytic Activity of Plasma-Sprayed Titania-Hydroxyapatite Coatings", Journal of Thermal Spray Technology, Vol. 16 (5-6), pp 776-782.

[7] Chen, M.A. Shan, L.M. and Hongtao, C. (2003), "Study on the Subsonic Speed Flame Spraying Coating of Hydroxyapatite", Rare Metals, Vol. 22(2), pp 116-120.

[8] Gaona, M. Lima, R.S. and Marple, B.R. (2007), "Nanostructured Titania/Hydroxyapatite Composite Coatings Deposited by High Velocity Oxy-Fuel (HVOF) Spraying", Materials Science and Engineering A, Vol. 458 (1-2), pp 141-149.

[9] Mohammadi, Z. Ziaei-Moayyed, A.A. and Sheikh-Mehdi Mesgar, A. (2007), "Grit blasting of Ti–6Al–4V alloy: Optimization and its effect on adhesion strength of plasma-sprayed hydroxyapatite coatings", Journal of Materials Processing Technology, Vol. 194, pp 15-23.

[10] Guehennec, L.L. Soueidan, A. Layrolle, P. and Amouriq, Y. (2007),"Surface treatments of titanium dental implants for rapid osseointegration", Dental Materials, Vol. 2 (3), pp 844-854.

[11] Sousa, S.R. and Barbosa, M.A. (1195), "The Effect of Hydroxyapatite Thickness on Metal Ion Release from Stainless Steel Substrates, Journal of Material Science: Materials in Medicine, Vol. 6, pp 818-823.

[12] Kumar, M.S. Mudali, U.K. and Rajeswari, S. (1994)," Investigation of failures in stainless steel orthopaedic implant devices: fatigue failure due to improper fixation of a compression bone plate", Journal of Material Science Letters, Vol. 13, pp 142-145.

[13] Fathi, M.H. Salehi, M. Saatchi, A. Mortazavi, V. and Moosavi, S.B. (2003), "In Vitro Corrosion Behaviour of Bioceramic, Metallic, and Bioceramic-Metallic, Coated Stainless Steel Dental Implants", Dental Materials, Vol. 19(3), pp 188-198.

[14] Lee, Y. P. Wang, C. K. Huang, T. H, Chen, C.C. Kao, C.T. and Ding, S.J. (2005), "In Vitro Characterization of Postheat-Treated Plasma-Sprayed Hydroxyapatite Coatings" , Surface & Coatings Technology, Vol. 197, pp 367- 374.